Eur. Phys. J. D **11**, 137–141 (2000)

THE EUROPEAN PHYSICAL JOURNAL D

EDP Sciences

Pattern selection and stabilization in an annular CO_2 laser

M.L. Ramón[1], R. Meucci[2,a], M. Ciofini[2], A. Labate[2], and L. Calero[2]

[1] Dept. of Physics and Applied Mathematics, Universidad de Navarra, 31080 Pamplona, Spain
[2] Istituto Nazionale di Ottica, Largo E. Fermi 6, 50125 Firenze, Italy

Received 15 December 1999

Abstract. The formation and stabilization of spatio-temporal patterns in an annular CO_2 laser is studied. We give experimental and numerical evidence of the role of a small spatial perturbation (consisting of a thin metallic wire inserted in the optical cavity) in the selection and stabilization of patterns.

PACS. 42.55.-f Lasers – 42.65.Sf Dynamics of nonlinear optical systems; optical instabilities, optical chaos and complexity, and optical spatio-temporal dynamics – 42.65.-k Nonlinear optics

1 Introduction

Pattern formation and spatio-temporal dynamics are widely investigated in many different areas, including optics, hydrodynamics, granular media, and chemical reactions [1]. In particular, nonlinear optics provides excellent examples of this kind of phenomena in a large variety of systems, such as liquid crystals [2], atomic vapors [3], organic films [4], photorefractive materials [5], and wide aperture lasers [6–10]. Usually, in this type of systems, laser action occurs simultaneously for a considerable number of transverse modes characterized by large values of the radial and azimuthal indices; this leads to a complex spatio-temporal pattern difficult to be analyzed. Previous works performed using CO_2 lasers emitting annularly symmetric intensity distributions [9,10], have studied the role of infinitesimal symmetry imperfections of the system on the observed spatio-temporal dynamics. Huyet *et al.* [9] gave evidence of their influence on the dynamics of structures with high azimuthal index. On the other hand, Labate *et al.* [10] analyzed the case of patterns with small azimuthal index near threshold, whose temporal behaviour was theoretically explained as a Takens-Bogdanov bifurcation. Both of them reported transitions between different patterns, as well as temporal oscillations of the intensity in some structures: periodic oscillations in [9], and aperiodic fluctuations determined by noise in [10].

Further interesting aspects of this symmetry can be investigated if the annular geometry is selected by using a toroidal mirror as one of the cavity mirrors. This solution provides a stable resonator, whereas the stability condition is not always fulfilled in a spherical resonator when spatial filters in the form of circular obstructions are inserted on the optical axis. With regard to the spatial structures, the annular configuration with toroidal mirror enables laser action for those families of patterns preserving the resonator symmetry, among all the modes present in a wide aperture laser. Furthermore, when the ratio of the external to the internal torus diameter is sufficiently close to one, there is only one relevant geometrical variable, namely, the azimuthal one. In this way, quasi one-dimensional patterns with periodical boundary conditions can be obtained. Finally, concerning the spatio-temporal evolution, the annular cavity gives the possibility of studying interesting phenomena, such as the highly irregular behaviours which can emerge when two or more patterns with different (and large) azimuthal indices coexist.

In this framework, we propose a pattern selection method based on the introduction of a weak spatial perturbation in the optical cavity. This technique, recently suggested by Wang *et al.* [11], achieves the selection and stabilization of two-dimensional patterns. In our particular case, the spatial perturbation consists of a thin metallic wire introduced in the optical cavity. Being the diameter of the wire a few times the laser wavelength, it acts as a diffracting obstacle which influences the eigenvalues of the different cavity modes. This method has been successfully implemented in wide aperture CO_2 lasers to select and stabilize hexagonal patterns [12]. Of course, the use of periodic spatial perturbations with no time dependence is by no means a method for controlling chaos in the sense originally proposed by Ott *et al.* [13] and later extended to the spatial-time domain [14]. However, it is useful whenever the system dynamics evolves on so fast time scales that a feedback can not be implemented.

Summarizing, we report on temporal evolution, selection and stabilization of annular patterns with high azimuthal index, in a CO_2 laser with a toroidal mirror. The paper is organized as follows: in Section 2, the experimental setup is described, and the experimental results presented. These experimental results are confirmed by numerical simulations, performed following the Fox and

[a] e-mail: ric@ino.it

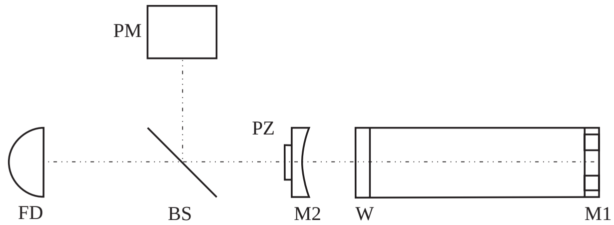

Fig. 1. Outline of the experimental setup. From right to left: M1 = toroidal mirror, W = transparent window, M2 = outcoupler, PZ = piezo translator, BS = beam splitter, PM = power meter, and FD = fast detector.

Li procedure [15]; the numerical results are reported in Section 3. Finally, conclusions are drawn in Section 4.

2 Experimental setup and results

The experimental setup is sketched in Figure 1. It consists of a wide aperture CO_2 laser with a Fabry-Perot configuration. The pyrex discharge tube of the laser (50 cm length, 3.54 cm internal diameter) is closed at one end by an antireflection ZnSe flat window (99.5% transmittance at normal incidence) and at the other end by a toroidal copper mirror (1150 mm radius of curvature; the external and internal diameters of its reflective part are 26 mm and 8 mm, respectively).

A spherical ZnSe outcoupler (38 mm diameter, 3 m radius of curvature, 90% reflection) closes the 87-cm-length Fabry-Perot cavity. This outcoupler is mounted on a piezo translator in order to adjust the cavity detuning.

The pumping of the active medium (4.5% CO_2, 82% He, 13.5% N_2, at an average pressure of 25 mbar) is provided by a high-voltage DC discharge. The electrodes have been purposely designed to preserve the cylindrical symmetry of the cavity.

A power meter and a $Hg_xCd_{1-x}Te$ fast detector have been used to measure the power of the output beam and its temporal evolution in a given point of the pattern, respectively.

In order to estimate the number of modes sustained by the cavity, we have to consider an "equivalent Fresnel number" suitable for the annular geometry of our system. Annular resonators have been analyzed for the case where the ratio between the internal and external radii of the mirror ($r_\mathrm{i}/r_\mathrm{e}$) is very close to one [16]. Under this condition, the resonator is equivalent to an infinite strip resonator, where the radial and azimuthal variables are uncoupled. Such an approximation can not be applied to our system: indeed, we have experimentally observed that the mean diameter of the patterns increases with the number of lobes. A rough estimation of the Fresnel number in our configuration could be $(r_\mathrm{e}^2 - r_\mathrm{i}^2)/\lambda L$ (λ = wavelength of the laser, L = cavity length) that, being over 16, assures the presence of a considerable amount of cavity modes.

The annular symmetry of the laser determines the geometry of the resulting patterns. Continuous rings have been observed, as well as discrete structures formed by an even number of lobes, and patterns showing both continuous and discrete contributions. In our experimental situation, the number of lobes varies from 22 to 36. Some of these structures are shown in Figure 2, where it can be noticed that the diameter of the patterns increases with the number of lobes.

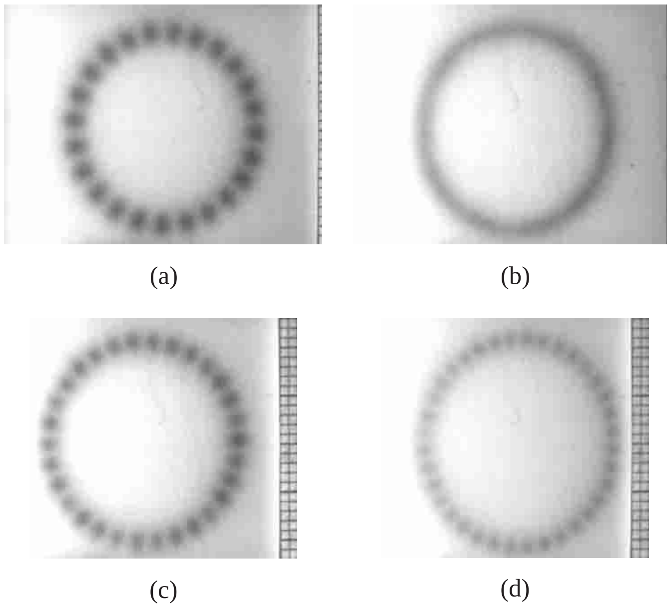

Fig. 2. Images of experimental patterns obtained on a thermal image plate placed at 11 cm from the outcoupler. (a) 24-lobe pattern, whose diameter is about 20 mm; (b) continuous pattern related to the previous structure (with the same diameter); (c) 32-lobe pattern; (d) 36-lobe pattern: the diameter has increased to near 22 mm.

Using the $Hg_xCd_{1-x}Te$ fast detector, we have verified that both continuous and discrete structures can display oscillating and non-oscillating behaviours, the former with frequencies ranging from 20 to 200 kHz approximately. This kind of oscillations have been already reported in previous works [7–10], where the patterns were interpreted as superpositions of azimuthal traveling waves (TW). Left- and right-azimuthal TW with the same amplitude give rise to pure standing-wave (SW) patterns, showing a multi-lobe configuration. When these two TW have different amplitudes, they can lead to a mixed structure consisting of a continuous ring (TW) with a superimposed multi-mode pattern, that can present temporal oscillations. The laser emission has been found to be linearly polarized. This fact simplifies theoretical approximations to the problem, allowing the use of scalar formulations.

In order to characterize the laser behaviour, we have varied the cavity detuning (Fig. 3). Without any external perturbation, when the resonance condition corresponding to the maximum output intensity is approached, the discrete 24-lobe pattern loses its stability and we observe the appearance of a continuous pattern or the superposition of both. A further increase of the cavity detuning leads (once surpassed the maximum) to the condition where competition with other modes, and consequently temporal instabilities appear. The data of Figures 4a and 4b

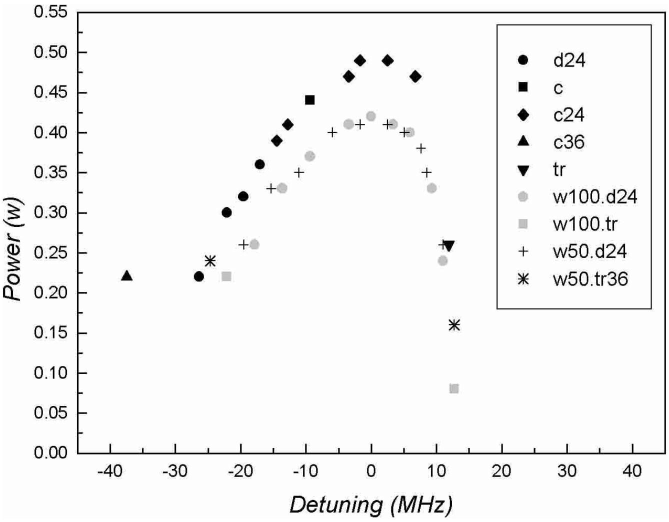

Fig. 3. Stability curves obtained for a current of 14.5 mA, at an average pressure of 25.5 mbar. The three curves are represented for detuning displacements from the position of the maximum intensity: the first one (black-filled symbols) has been obtained without perturbations, and the other two with wires of 100 (gray-filled symbols) and 50 μm (+ and $*$ symbols), respectively. Legend notation: (wx.)l(n), where wx. = with a x μm-diameter wire (just in case there is a wire); l = d (discrete), c (continuous), tr (transitions between more than two patterns); $n =$ number of lobes of the pattern, cn = n lobes superimposed to a continuous pattern.

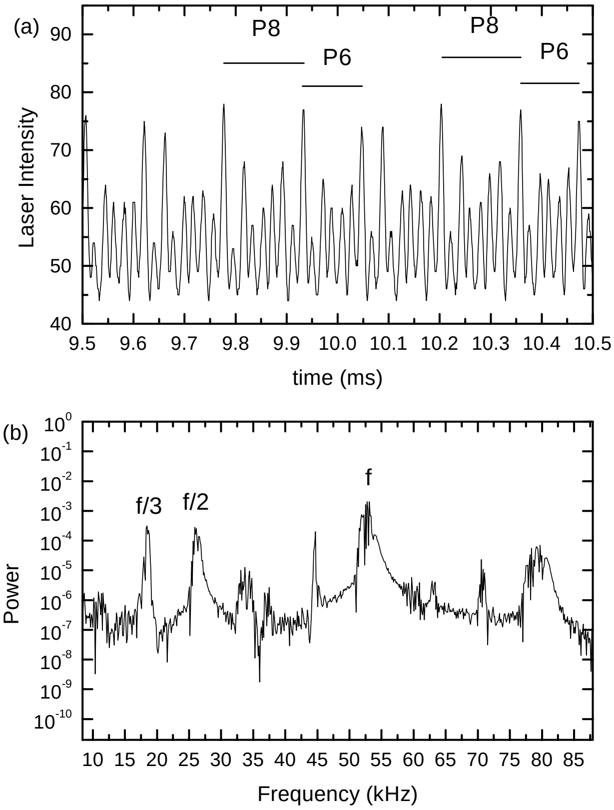

Fig. 4. Irregular behaviour resulting from interactions between more than two multi-lobe patterns. (a) Strongly irregular oscillations showing period windows P6 and P8. (b) Power spectrum showing the fundamental frequency ($f \approx 53$ kHz) together with subharmonic peaks at $f/3$ and $f/2$.

were recorded during the interaction between more than two different multi-lobe patterns: Figure 4a shows the irregular behaviour of the intensity in a point of the pattern, whereas in the corresponding power spectrum of Figure 4b, it can be noticed the presence of subharmonics of the fundamental frequency.

The selection of multi-lobe patterns, and hence the disappearance of the continuous distribution and even of irregular behaviours, can be forced by making use of a thin metallic wire (50 or 100 μm diameter, placed 11 cm far from the outcoupler inside the cavity). As can be seen in Figure 3, the introduction of the wire enlarges considerably the range of stability of the 24-lobe mode, introducing only nearly negligible “side effects” such as small intensity losses (5–10%). Another effect is a slight displacement (smaller than 10 MHz) in the detuning value related to the maximum intensity, that has been corrected in the figure by shifting the curves in order to place the maxima for the same detuning value. Notice that the selected pattern remains stable approximately in the same range where the different versions of the structure (discrete or continuous, with or without oscillations) were present before the insertion of the spatial perturbation. Moreover, the weak spatial perturbation does not give rise to new patterns, or to modified versions of the previously observed ones; indeed, it stabilizes the same multi-lobe modes observed without the wire. Furthermore, concerning the temporal evolution, this method assures the elimination of temporal oscillations in the resulting patterns, and even in the transitions between them. Thus, the stability domain of the multi-lobe mode is extended up to the appearance of another laser mode with a different azimuthal index, avoiding irregular temporal regimes.

Finally, it is interesting to remark that the insertion of masks with a different number of wires in diametrical positions enables the selection of more specific patterns, namely, those whose lobe-number is a multiple of the number of radial obstacles in the mask [11,12]. For example, the insertion inside the optical cavity of a mask of 6 equidistant radial partitions (3 wires of 50-μm diameter at 60°), leads to the stabilization of 24-, 30- or 36-lobe patterns; whereas a mask of 7 wires (14 angular partitions) enables only the presence of the 28-lobe pattern.

3 Numerical analysis

A numerical analysis based on the Fox and Li method [15] confirms the previous results. The simulations have been performed adopting exactly the same geometrical configuration of the experiment. The transverse plane is represented by a square grid of 512×512 pixels (with 100-μm-width pixels) and propagation within the laser cavity has been accounted for *via* Fourier transforms [17]. We also neglected the dynamical behavior of the active medium,

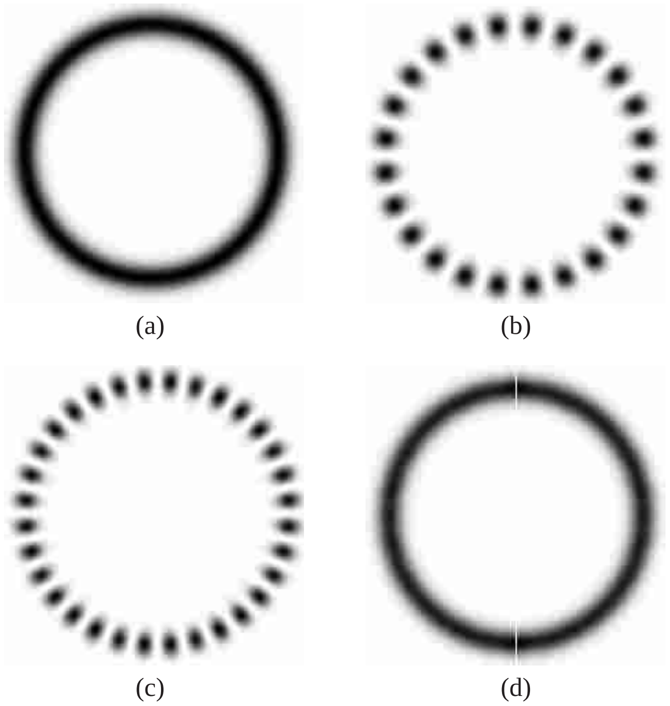

Fig. 5. Numerical simulations. Representation of the transverse-plane intensity of the output beam (after 500 round trips) for the following initial conditions: (a) uniform intensity and phase distributions. Losses = 0.005%. (b) Uniform intensity, and phase alternating between 0 and π in 24 equal angular sectors. Both with and without the wire, the resulting pattern (the 24-lobe one) and the losses (0.12%) are the same. (c) 32-lobe structure reproduced using the same method (with 32 angular sectors), with or without the wire. Losses = 0.26%. (d) Uniform intensity and phase distribution. The effect of a 1-pixel obstacle is included. The continuous pattern is not exactly reproduced. The losses in the new structure are 0.74%.

replacing it with a constant amplification factor. On the one hand, such an approximation does not allow to study the effect of the detuning (and thus different cavity eigenmodes are selected in our calculations by appropriately choosing the initial condition for the laser intensity and phase distributions). On the other hand, like in the experiment (where a diffractive perturbation was introduced in a well defined transverse plane), interesting results can be obtained on the role played by the wire in changing the cavity eigenvalues of individual eigenmodes.

The numerical results are summarized in Figure 5 (convergence has been always reached after 500 cavity round trips). Starting with intensity and phase uniformly distributed in the transverse plane as initial conditions, the continuous pattern is found, with uniform phase distribution (see Fig. 5a); the calculated cavity losses, that is, the mode eigenvalue, for this configuration are 0.005%. The 24-lobe pattern can be studied with initial uniform intensity distribution, and phase set alternately to zero and π in 24 equal angular-sectors (see Fig. 5b). In this case, cavity losses equal to 0.12% have been obtained. Similar structures with a different number of lobes can be simulated by changing the number of partitions in the initial phase distribution (see Fig. 5c, consisting of 32 lobes, with losses reaching 0.26%). Note that the above per cent values are very small since, considering as ideal all optical elements, we have neglected most of the losses present in the experiment, such as non perfect reflectivity of the mirrors. Anyway, they are not relevant for our treatment because they are uniformly distributed in the transverse directions and thus do not contribute to mode selection. It is clear that, in a real unperturbed cavity where all the structures of Figure 5a and 5c are eigenmodes, the continuous distribution would be automatically selected since it exploits the lowest losses.

Next, a "wire" of one-pixel width (100 μm of diameter) has been included in the simulation algorithm. Initial homogeneous amplitude and phase distributions lead to the pattern shown in Figure 5d, that is, the continuous pattern splits into two parts. Anyway the cavity losses, clearly affected by the presence of the wire, reach 0.74%. On the contrary, the 24-lobe (n-lobe) mode maintains exactly the same cavity losses than without the wire. Thus, with the wire, this last pattern has lower losses than the one shown in Figure 5d, and it will be consequently preferred. Although a quantitative comparison with the diffraction losses of the experimental cavity is not possible, this result agrees with the observed selection of the multi-lobe patterns when weak spatial perturbations are introduced.

4 Conclusions

In this paper, we have reported on the formation and selection of patterns on an annular CO_2 laser. Continuous and discrete structures have been observed, as well as superpositions of both configurations. The highest power values correspond to the continuous, or continuous with lobes structures, whereas the discrete structures are formed when the cavity losses are increased.

We have verified that the introduction of a weak spatial perturbation inside the optical cavity (a metallic wire of 50 or 100 μm) selects and stabilizes a multi-lobe pattern, increasing its stability range and avoiding temporal oscillations. Concerning laser applications, the stabilization of patterns with azimuthal dependence does not represent a limitation on the uniformity when the beam is focused. A suitable phase-filtering process on the output beam can reduce the azimuthal modulation in the far-field distribution [18].

Numerical simulations based on the Fox and Li method, agree qualitatively with the experimental results.

This work was partially supported by the EC Contract FMRX-CT96-0010 of the coordinated project "Nonlinear dynamics and statistical physics of spatially extended systems". The authors would like to thank F.T. Arecchi and A. Lapucci for very helpful discussions. M.L.R. thanks the INO for the concession of a grant within the frame of this project and their kind hospitality, as well as the *Asociación de Amigos de la Universidad de Navarra* for their financial support.

References

1. M.C. Cross, P.C. Hohenberg, Rev. Mod. Phys. **65**, 851 (1993); P. Manneville, *Dissipative Structures and Weak Turbulence* (Accademic Press, San Diego, 1990); E.L. Koschmieder, *Bénard cells and Taylor vortices* (Cambridge University Press, Cambridge, 1994); special issue on *Transverse Effects in Optical Systems*, edited by N.B. Abraham, W.J. Firth, J. Opt. Soc. Am. B **7**, 951 (1990).
2. R. Macdonald, H.J. Eichler, Opt. Commun. **89**, 289 (1992); B. Thüring, R. Neubecker, T. Tschudi, Opt. Commun. **102**, 111 (1993).
3. G. Grynberg, E. Le Bihan, P. Verkerk, P. Simoneau, J.R.R. Leite, D. Bloch, S. Le Bioteux, M. Ducloy, Opt. Commun. **67**, 363 (1988); J. Pender, L. Hesselink, J. Opt. Soc. Am. B **7**, 1361 (1990).
4. J. Glückstad, M. Saffman, Opt. Lett. **20**, 551 (1995).
5. T. Honda, Opt. Lett. **18**, 598 (1993).
6. J.R. Tredicce, E.J. Quel, A.M. Ghazzawi, C. Green, M.A. Pernigo, L.M. Narducci, L.A. Lugiato, Phys. Rev. Lett. **62**, 1274 (1989); W.W. Rigrod, Appl. Phys. Lett. **2**, 51 (1963); D. Dangoisse, D. Hennequin, C. Lepers, E. Louvergneaux, P. Glorieux, Phys. Rev. A **46**, 5955 (1992).
7. R. López-Ruiz, G.B. Mindlin, C. Pérez-García, J.R. Tredicce, Phys. Rev. A **49**, 4916 (1994).
8. E.J. D'Angelo, E. Izaguirre, G.B. Mindlin, G. Huyet, L. Gil, J.R. Tredicce, Phys. Rev. Lett. **68**, 3702 (1992).
9. G. Huyet, C. Mathis, J.R. Tredicce, Opt. Commun. **127**, 257 (1996).
10. A. Labate, M. Ciofini, R. Meucci, S. Boccaletti, F.T. Arecchi, Phys. Rev. A **56**, 2237 (1997).
11. P.-Y. Wang, P. Xie, J.-H. Dai, H.-J. Zhang, Phys. Rev. Lett. **80**, 4669 (1998).
12. M. Ciofini, A. Labate, R. Meucci, P.-Y. Wang, Opt. Commun. **154**, 307 (1998); R. Meucci, A. Labate, M. Ciofini, P.-Y. Wang, Quant. Semiclass. Opt. **10**, 803 (1998).
13. E. Ott, C. Grebogi, J.A. Yorke, Phys. Rev. Lett. **64**, 1196 (1990).
14. W. Lu, D. Yu, R.G. Harrison, Phys. Rev. Lett. **76**, 3316 (1996); R. Martin, A.J. Scroggie, G.-L. Oppo, W.J. Firth, Phys. Rev. Lett. **77**, 4007 (1996).
15. A.G. Fox, T. Li, Bell Syst. Tech. J. **40**, 453 (1961).
16. M. Morin, P.-A. Bélanger, Appl. Opt. **31**, 1942 (1992).
17. J.W. Goodman, *Introduction to Fourier Optics* (McGraw-Hill, San Francisco, 1968).
18. A. Lapucci, M. Ciofini, Appl. Opt. **38**, 4552 (1999).